

# Factorial design of reactive concrete powder containing electric arc slag furnace and recycled glass powder

Joaquín Abellán-García <sup>a</sup>, Andrés Núñez-López <sup>b</sup>, Nancy Torres-Castellanos <sup>c</sup> & Jaime Fernández-Gómez <sup>d</sup>

<sup>a</sup> Facultad de Ingeniería Civil, Escuela Colombiana de Ingeniería Julio Garavito, Bogotá, Colombia. & Universidad Politécnica de Madrid, Madrid, España. [j.abellang@alumnos.upm.es](mailto:j.abellang@alumnos.upm.es)

<sup>b</sup> I&D, Cementos Argos SA, Medellín, Colombia. [anunezn@argos.com.co](mailto:anunezn@argos.com.co)

<sup>c</sup> Facultad de Ingeniería Civil, Escuela Colombiana de Ingeniería Julio Garavito, Bogotá, Colombia. [nancy.torres@escuelaing.edu.co](mailto:nancy.torres@escuelaing.edu.co)

<sup>d</sup> Departamento Ingeniería civil y Construcción, Universidad Politécnica de Madrid, Madrid, España. [jaime.fernandez.gomez@upm.es](mailto:jaime.fernandez.gomez@upm.es)

Received: October 3<sup>rd</sup>, 2019. Received in revised form: February 28<sup>th</sup>, 2020. Accepted: March 9<sup>th</sup>, 2020

## Abstract

The main objective of this research is to develop an optimized mixture of reactive powder concrete (RPC) containing supplementary cementitious materials (SCM), such as Electric Arc Slag Furnace (EASF), and Recycled Glass Powder (RGP) among others, through a factorial design. Accurate polynomial regressions were adjusted between considered factors and obtained responses such spread flow and compressive strength at different ages of the concrete. A multi-objective algorithm was executed to reach an eco-friendly mixture with the proper flow, the highest compressive strength, while simultaneously having the minimum content of cement. The experimental verification of this mathematical optimization demonstrated that the use of 621 kg/m<sup>3</sup> of ASTM Type HE cement, with a maximum content of 100 kg/m<sup>3</sup> of silica fume, should be considered the most appropriate amount to be employed in the RCP mixture to achieve a value of compressive strength over 150 MPa and a self-compacting mixture.

**Keywords:** RPC; sustainability; EASF; RGP; compressive strength; RSM; optimization.

# Diseño factorial de concretos de polvos reactivos conteniendo escoria de arco eléctrico y polvo de vidrio reciclado

## Resumen

El objetivo principal de esta investigación es desarrollar una mezcla optimizada de concreto de polvos reactivos (RPC) que contenga materiales cementicios suplementarios (SCM), como la escoria siderúrgica de arco eléctrico (EASF) y el polvo de vidrio reciclado (RGP) entre otros, utilizando el diseño factorial. Se calcularon diferentes regresiones polinómicas para predecir con precisión las variables respuesta (flujo estático y resistencia a compresión a distintas edades) en función de los factores considerados. A través de un algoritmo multiobjetivo, se determinó la mezcla que alcance la resistencia y flujo estático adecuados con un contenido mínimo de cemento. La verificación experimental de esta optimización matemática mostró que con 621 kg/m<sup>3</sup> de cemento ASTM Tipo HE, y un contenido máximo de 100 kg/m<sup>3</sup> de humo de sílice, se puede alcanzar una resistencia a compresión superior a los 150 MPa en un concreto, además, autocompactante.

**Palabras clave:** RPC; sostenibilidad; EASF; RGP; resistencia a compresión; RSM; Optimización.

## 1. Introduction

Concrete is the most popular material in civil engineering. Its applications include buildings, industrial structures, bridges and dams. Every day the concrete is improving, to

reach better characteristics. In this line, French Company BOUYGUES first developed a new type of ultra-high-performance cement based composite material—known as reactive powder concrete (RPC)—with ultra-high compressive strength due to its ultra-dense structure [1,2].

**How to cite:** Abellán-García, J., Núñez-López, A., Torres-Castellanos, N. and Fernández-Gómez, J. Factorial design of reactive concrete powder containing electric arc slag furnace and recycled glass powder. DYNA, 87(213), pp. 42-51, April - June, 2020.



© The author; licensee Universidad Nacional de Colombia. Revista DYNA, 87(213), pp. 42-51, April - June, 2020, ISSN 0012-7353  
DOI: <http://doi.org/10.15446/dyna.v87n213.82655>

Improved durability is another feature of RCP [3,4]. This material, presented in the 90's by Richard and Cheyrezy [1], contains over 800 kg/m<sup>3</sup> of Portland cement (C), and high amounts of silica fume (SF), quartz powder (QP), silica sand (SS) with a maximum size of 600 µm, high-range water reducers polycarboxylate-ether-based superplasticizers (PCE), and sometimes steel fiber [1,5,6]. In recent years, RPC has already been successfully applied in the field of engineering construction, due to its high mechanical properties and excellent durability.

However, because of the high contents of cement, quartz sand, and silica fume used, the cost of RPC is considerably higher than conventional concrete, which limits the extent of its application [7]. Therefore, considering that the high cost of RPC is a disadvantage that restricts its wider usage, some supplementary cementitious materials such as limestone powder (LP) and industrial by-products such as ground granulated blast-furnace slag (GGBFS), fly ash (FA), and glass powder (GP), *inter alia*, have been used as partial cement replacements. For example, the influence of the contents of blast furnace slag (BFS) on the microstructural and mechanical properties of RPC was investigated [8]. Mixtures exceeding 150 MPa of compressive strength had cement contents between 680 and 977 kg/m<sup>3</sup>. Another research [9] showed some mechanical investigation on RPC with around 650 kg/m<sup>3</sup> cement, 420 kg/m<sup>3</sup> GGBFS and 120 kg/m<sup>3</sup> silica fume. Incorporating limestone powder in RPC improved the hydration process at the early-age, producing denser particle packing, and improving mechanical properties [10]. Other study used nano-CaCO<sub>3</sub> as a component of binder [11]. It was observed a 17 % increase in compressive strength compared to the control specimens without nano-CaCO<sub>3</sub>. The behavior of dosages of RPC containing fly ash (FA), silica fume (SF) and fluid catalytic cracking residue (FC3R), a by-product of the crude oil industry, was analyzed [12,13]. The research showed the possibility of a partial replacement of cement and silica fume. However, the necessary amount of cement to reach 150 MPa compressive strength was higher than 740 kg/m<sup>3</sup>. Several researchers have reported their test results about the possibility of using rice husk ash (RHA) to replace silica fume (SF) in producing RPC [14,15]. The experimental results showed that the compressive strength of RPC incorporating RHA reaches more than 150 MPa. The results of the partial substitution of silica fume with fine glass powder (FGP) in RPC were analyzed [16]. The results demonstrated that compressive strength values of 235 and 220 MPa under 2 days of steam curing can be achieved when replacing 30% and 50% of SF with FGP respectively, with a mean particle size ( $d_{50}$ ) of 3.8 µm. However, the amount of cement used exceeded 800 kg/m<sup>3</sup>. Also recycled glass powder was used to replace quartz sand, cement and quartz powder particles [5,17]. Even a RPC incorporating waste bottom ash (WBA) was developed [18]. The results showed that due to the existence of the metallic aluminum particles in WBA, the mechanical properties of the concrete could be reduced. None of the dosages reached a compressive strength of 150 MPa. These investigations show that it is possible to replace significant amounts of cement

and silica fume in RPC dosages with other less expensive and more sustainable components without significantly affecting the compressive strength. However, how to find a reasonable balance between the proportion of these supplementary cementitious materials in the binder and the mechanical and rheological properties of RPC still remains an open question.

Furthermore, Portland cement, the principal hydraulic binder used worldwide in modern concrete, is not only a product of an energy-intensive industry (4 GJ/ton of cement) but also responsible for large emissions of CO<sub>2</sub>, thereby contributing to global warming. Manufacturing one ton of Portland-cement clinker releases nearly one ton of CO<sub>2</sub> into the atmosphere, while nowadays the world's yearly cement output of 1.5 billion tons of mostly Portland cement is responsible for nearly 7% of the global CO<sub>2</sub> emissions [14]. Hence, one of the key sustainability challenges is to design and produce concrete with less clinker and inducing lower CO<sub>2</sub> emissions than a traditional one, while providing the same reliability, and better durability. The RPC seems to be one of the candidates to reduce the global warming impact of construction materials. This is because it allows for thinner sections thanks to its excellent mechanical behavior. However, as shown before, when producing RPC, the cement or binder content is always relatively high [19]. This is why the partial replacement of cement in RPC, especially when made by locally available industrial by-products, is of great interest to the scientific community [3].

While striving towards a cost-effective and more sustainable RPC, the objective of this study is to effectively design and produce RPC with low cement amounts, with a maximum content of silica fume of 100 kg/m<sup>3</sup>. The design of the concrete mixtures is based on the aim of achieving compressive strength and rheological properties with minimum amounts of cement through a 3-factor Design of Experiments (DoE). To ensure a densely compacted cementitious matrix, the modified Andreasen & Andersen particle packing model ( $A \& A_{mod}$ ) [20] was used. Cementitious supplementary materials such as limestone powder, electric arc slag furnace and recycled glass flour were used as a partial replacement for cement and silica fume in the concrete.

In this work is presented a factorial-design procedure for reactive powder concrete (RPC) composite material with compression strength up to 150 N/mm<sup>2</sup>, with the minimum amount of cement possible, while using limestone powder (LP), recycled glass powder (RGP) and electric arc slag furnace (EASF) as partial substitution of cement and silica fume. For the mathematical optimization a multi-objective simultaneous optimization R-coded algorithm [21] was adopted. Finally, the mathematical-selected mixture was verified with experimental work.

## 2. Materials and methodology

### 2.1. Materials

The RPC mixtures were prepared with raw materials locally available in Colombia. ASM Type HE cement (C)

was used. The HE cement had a specific gravity of 3.15, and mean particle diameter ( $d_{50}$ ) of 8  $\mu\text{m}$ . The SF used in the mixture proportioning complied with ASTM C-1240 specifications and had a specific gravity of 2.20 and  $d_{50}$  of 0.15  $\mu\text{m}$ . The RPC was also designed with a SS of a specific gravity of 2.65, maximum particle size ( $d_{max}$ ) of 600  $\mu\text{m}$ , and  $d_{50}$  of 165  $\mu\text{m}$ . RGP with a specific gravity of 2.55 and  $d_{50}$  of 28  $\mu\text{m}$  was used, LP with a specific gravity of 2.73 and  $d_{50}$  of 2  $\mu\text{m}$ , and EASF with a specific gravity of 3.15 and  $d_{50}$  of 2.1  $\mu\text{m}$  were used as supplementary cementitious materials. EASF and RGP with the particle size distribution (PSD) depicted in Fig. 1 were obtained by grounding locally available raw waste materials with a jet mill to different degrees of fineness, by applying different grinding speeds. Table 1 shows the chemical composition of the materials used in this study. Fig. 1 provides the particle size distribution (PSD) of the cement, SF, EASF, RGP and

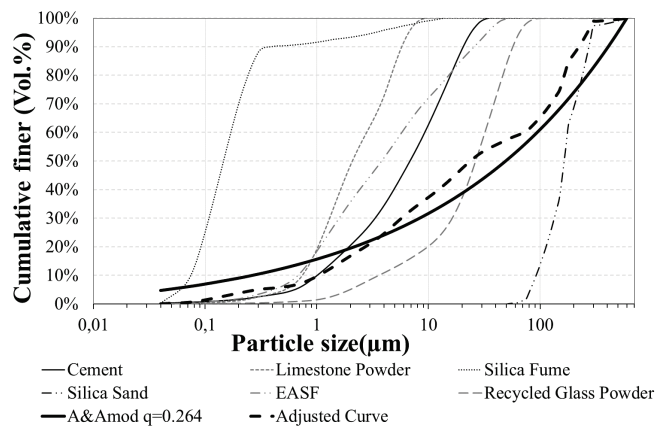


Figure 1. Particle size distribution of the used materials.  
Source: The Authors.

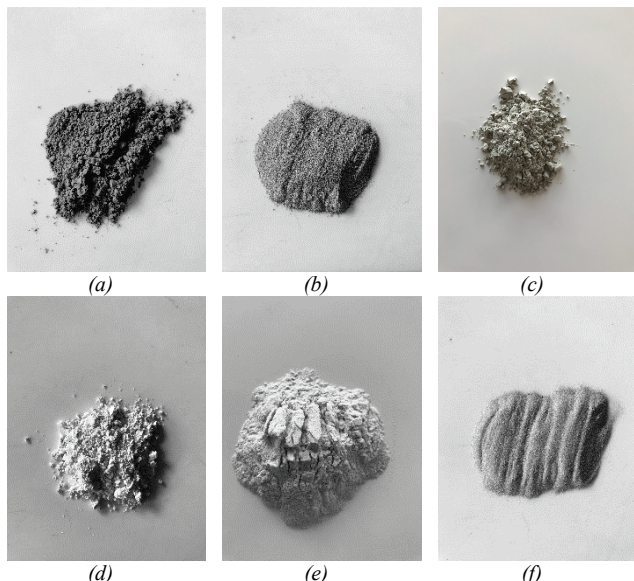


Figure 2. Materials used in this research: (a) Cement HE; (b) condensed silica fume; (c) EASF; (d) micro limestone powder; (e) recycled glass powder; and (f) silica sand.  
Source: The Authors.

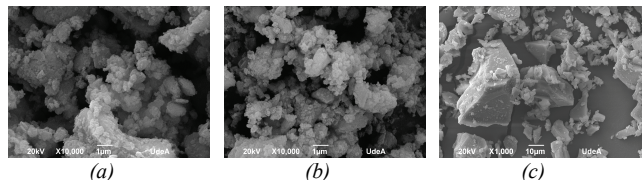


Figure 3. FSEM of supplementary cementitious materials used in research: (a) EASF; (b) Limestone powder; and (c) RGP.  
Source: The Authors.

Table 1.  
Chemical properties of materials.

Chemical analysis	OPC	SF	EASF	LP	RGP	SS
SiO <sub>2</sub> %	19.42	92.29	21.70	0.90	72.89	95.80
Al <sub>2</sub> O <sub>3</sub> %	4.00	0.59	6.20	0.10	1.67	0.11
CaO%	64.42	3.89	33.13	55.51	9.73	0.38
MgO%	1.52	0.26	10.60	0.70	2.08	0.20
SO <sub>3</sub> %	1.93	0.07	1.14	0.10	0.01	0.52
Na <sub>2</sub> O%	0.19	0.31	0.15	0.03	12.54	0.25
K <sub>2</sub> O%	0.39	0.54	0.03	0.00	0.76	3.49
TiO <sub>2</sub> %	0.38	0.01	0.42	0.00	0.04	0.25
Mn <sub>2</sub> O <sub>4</sub> %	0.05	0.01	1.98	0.01	0.01	0.01
Fe <sub>2</sub> O <sub>3</sub> %	3.61	0.24	18.92	0.05	0.81	0.09
Loss of ignition %	2.58	0.60	4.67	42.21	1.00	0.31
Specific gravity (gr/cm <sup>3</sup> )	3.16	2.20	3.15	2.73	2.55	2.65

Source: The Authors.

SS. Fig. 2 shows a photograph of the raw materials used in the research. A polycarboxylate (PCE)-based superplasticizer with a specific gravity of 1.07 and solid content of 40% was used.

The supplementary cementitious materials (EASF, LP and RGP) used as partial substitution of cement and silica fume were analyzed by scanning electron microscopy (SEM) as depicted in Fig. 3. Results point out the lack of porosity of the recycled glass powder.

## 2.2. Preparation and test of specimens

The amount of cement, water, and superplasticizer were established by the DoE. The other components were ruled by the  $A\&A_{mod}$  using a  $q$  value of 0.264, according to eq. (1).

$$P_{tar}(D) = \frac{(D^q - D_{min}^q)}{(D_{max}^q - D_{min}^q)} \quad (1)$$

where  $D$  is the particle size,  $P_{tar}(D)$  is the weight fraction of total solids that are smaller than  $D$ ,  $D_{max}$  and  $D_{min}$  are the maximum and minimum particle sizes, respectively, and  $q$  is the Distribution Modulus. The  $q$  value determines the ratio of aggregate/cementitious paste content needed for achieving the densest possible particle packing, which likely achieves the greatest compressive strength. A lower value of  $q$  implies a high content of cement and SF, increasing the packing density and strength but also the final cost of concrete. The value of  $q$  was determined in a previous research [22].

After the dosage was established, a liner mortar mixer was used to produce the concrete. At the end of mixing, the fresh properties of the UHPC mixtures were measured to determine the static slump flow diameter in accordance with ASTM C1437 specifications [23] by taking the spread diameter of the mini-slump cone in the flow-table test, filling the truncated conic mold with the concrete and lifting it away. The spread flow of the concrete ( $\mathcal{O}_m$ ) was obtained as the average diameter of the measure in four perpendicular directions.

After performing the static flow test, the concrete was cast in 50 mm cube molds. To improve the packing density of concrete a vibrating table was used after pouring the molds. The samples were demolded approximately 24 h after casting, and then cured in a moisture room at 20 °C until the day of the test. Concrete compression machine with 3000 KN in capacity was used, following ASTM C109 [24]. For each different age, i.e. 24 hours, 7 days, and 28 days, three samples were tested.

### 2.3. Response Surface Analysis (RSM)

The response-surface methodology comprises a body of methods for the exploring of optimum operating conditions through experimental methods [25]. It is a collection of mathematical and statistical techniques for the modeling and analysis of problems based on the statistical design of experiments and least square error fitting. It is used extensively where several input variables influence the process [26]. RSM usually involves an experimental design, a response surface model and an optimization [27,28].

A Central Composite Design (CCD), an efficient experimental design, was chosen for its ability to estimate second-order effects, to analyze a response surface with a relatively small number of trials, to determine the interrelationships between factors, to model the response data, and to locate the optimal response [29]. The second-order model is widely used in this methodology for the following reasons: (i) the quadratic model is very flexible as an approximation to the real response surface. It can take on a wide variety of functional forms, so it will usually work as an approximation to the real response surface; (ii) it is not complicate to estimate the parameters - the  $a$ 's in eq.(3) - in the second-order model; and (iii) there is considerable amount of experience indicating that second-order models work well in solving real response surface problems.

A central composite design is the most commonly used response surface designed experiment. Central composite designs are a factorial or fractional factorial design with center points, augmented with a group of axial points (also called star points) which increase the variable space and allow for the estimation of the second-order terms. The design used in this work involves  $2^N$  factorial points (which are in the corners of cube),  $2N$  axial points at a distance  $\pm \alpha$  from the origin and 4 central point, as depicted in Fig. 4. Hence, a total of 18 set point, 4 center points (2 Axial plus 2 Cube), 2 blocks (Cube and Axial) and  $\alpha = \pm 1.78885$ , was used in this research.

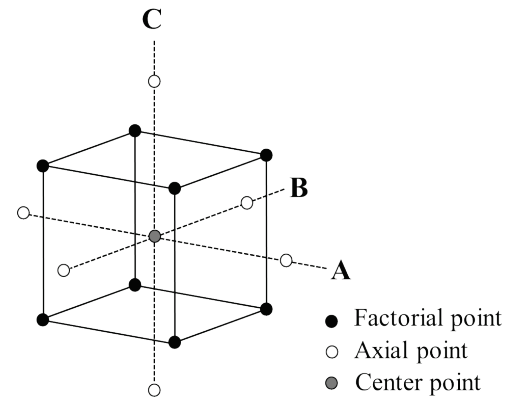


Figure 4. Central Composite Design for 3 design variables at 2 levels  
Source: The Authors.

Table 2.  
Factors and range of variation.

Factor	Coded	Range of variation				
		-1.789	-1	0	1	1.789
Cement (kg/m <sup>3</sup> )	A	580.280	600.000	625.000	650.000	669.720
w/b	B	0.156	0.160	0.165	0.170	0.174
HRWR(%vol)	C	1.840	2.000	2.200	2.400	2.560

Source: The Authors.

The statistical analysis was carried out on the coded data sets in order to simplify the interpretation of the results. The coding was as according to eq. (2).

$$X_j = (Z_j - Z_{0j}) / (Z_{maxj} - Z_{minj}) \quad (2)$$

where  $X_j$  is the coded value of factor  $j$ ,  $Z_j$  is the real value of factor  $j$ ,  $Z_{0j}$  is the real value of factor  $j$  at the center point and  $Z_{maxj}$  and  $Z_{minj}$  are the maximum and minimum values of the factor  $j$  in the domain space respectively.

To estimate each response a second-order polynomial equation calculated according to eq. (3) was used.

$$Y = a_0 + \sum a_i x_i + \sum a_{ii} x_i^2 + \sum a_{ij} x_i x_j \quad (3)$$

where  $Y$  was the estimate of the response (i.e. dependent variable),  $a_0$  is the overall mean response,  $a_i$  are linear coefficients,  $a_{ii}$  are quadratic coefficients,  $a_{ij}$  are coefficients of the interaction, and  $x_i$ ,  $x_j$  represent the factors (i.e. independent variables). The factors defined for this experiment are fixed at the levels shown in Table 2.

In this work, three independent factors, namely, cement content in kg/m<sup>3</sup>, water binder ratio (w/b), and volume of superplasticizer to total dosage ratio (PCE), were chosen. To determine the proportion of the rest of the concrete components, the  $A\&A_{mod}$  curve was used. Four responses were also considered, including compressive strength with standard curing conditions at 24 hours (R1), 7 days (R7), 28 days (R28), and spread flow ( $\mathcal{O}_m$ ).

### 3. Results and discussion

#### 3.1. Adjusted model and validation

In this research, a central composite design with 18 design points was chosen to fit the response in domain space for the 3 design variables at 3 levels. Table 3 presents the factorial set point combinations and their corresponding values obtained experimentally. R, a language and environment for statistical computing [30], for experiment design and analysis, was used to plan the experiment.

The corresponding mixture proportions of this DoE, adjusted according to the  $A\&A_{mod}$  curve, are presented in Table 4.

The  $\bar{\varnothing}_m$  parameter was measured on spread test and calculated according to eq. (4), in which:  $\bar{\varnothing}_i$  is the mean value for each  $i$  of the four perpendicular diameters, in mm.

Table 3.  
The set point combinations and the corresponding experimental responses.

Run	A	B	C	$\bar{\varnothing}_m$ (mm)	R1 (MPa)	R7 (MPa)	R28 (MPa)
1	-1	-1	-1	221.25	27.01	104.72	139.84
2	1	-1	-1	203.00	40.84	77.56	100.68
3	-1	1	-1	265.00	46.27	105.38	134.84
4	1	1	-1	256.50	56.18	118.14	134.62
5	-1	-1	1	245.75	45.93	121.55	148.72
6	1	-1	1	219.00	45.81	99.93	127.29
7	-1	1	1	274.00	24.20	83.28	141.05
8	1	1	1	264.25	9.90	90.66	156.42
9	0	0	0	247.75	47.72	79.99	143.51
10	0	0	0	240.25	47.81	96.93	123.65
11	-1.789	0	0	239.00	27.78	101.70	140.00
12	1.789	0	0	261.00	50.67	107.60	148.00
13	0	-1.789	0	203.50	46.84	97.44	129.76
14	0	1.789	0	278.75	40.63	110.24	162.64
15	0	0	-1.789	233.50	52.49	113.93	153.86
16	0	0	1.789	250.75	18.24	94.63	154.54
17	0	0	0	239.25	39.39	98.54	142.92
18	0	0	0	231.00	37.38	76.73	152.84

Source: The Authors.

Table 4.  
Proportion of mixing components expressed as a function of the weight of the cement.

Run	C	SF	EASF	GPF	MLP	PCE	SS	w/b
1	1	0.167	0.625	0.117	0.083	0.036	1.552	0.160
2	1	0.154	0.492	0.069	0.077	0.033	1.510	0.160
3	1	0.167	0.625	0.117	0.083	0.036	1.499	0.180
4	1	0.154	0.492	0.069	0.077	0.033	1.463	0.180
5	1	0.167	0.625	0.117	0.083	0.043	1.548	0.160
6	1	0.154	0.492	0.069	0.077	0.040	1.506	0.160
7	1	0.167	0.625	0.075	0.083	0.043	1.553	0.180
8	1	0.154	0.492	0.069	0.077	0.040	1.459	0.180
9	1	0.160	0.540	0.084	0.080	0.038	1.539	0.170
10	1	0.160	0.540	0.084	0.080	0.038	1.539	0.170
11	1	0.172	0.646	0.121	0.086	0.041	1.625	0.170
12	1	0.149	0.449	0.075	0.075	0.035	1.434	0.170
13	1	0.160	0.540	0.084	0.080	0.038	1.583	0.150
14	1	0.160	0.540	0.084	0.080	0.038	1.495	0.190
15	1	0.160	0.540	0.084	0.080	0.032	1.543	0.170
16	1	0.160	0.540	0.084	0.080	0.044	1.535	0.170
17	1	0.160	0.540	0.084	0.080	0.038	1.539	0.170
18	1	0.160	0.540	0.084	0.080	0.038	1.539	0.170

Source: The Authors.

Table 5.  
Results for developed regression models.

Response	R2	Adj-R2	RMSE	F-Stat	Lack of fit	P-value	Shapiro P-value
$\bar{\varnothing}_m$	0.971	0.955	3.52	60.58	4.50	<0.0001	0.966
R1	0.965	0.934	2.30	31.16	3.26	<0.0001	0.629
R7	0.957	0.909	2.00	19.80	3.00	<0.0001	0.679
R28	0.955	0.930	1.46	38.67	1.87	<0.0001	0.472

Source: The Authors.

$$\bar{\varnothing}_m = \frac{1}{4} \sum_{i=1}^4 \bar{\varnothing}_i \quad (4)$$

According to eq. (3) a quadratic polynomial regression model was adjusted for each response (R1, R7, R28, and  $\bar{\varnothing}_m$ ). There were two steps involved in this process: first calculating a proper model, and then verifying the accuracy of the selected model. In this study, a backward stepwise process was used to achieve an accurate model for each response. It starts with the full second-order polynomial model, eq. (3), performed to estimate the relationship between the variables and the responses based on experimental results from CCD. Then, the process is followed by removing the variable with the largest P-value. The procedure continues until only those variables which are significant (P-value < 0.05) remain in the model. Once the non-significant term was removed, the adjusting model process is repeated until all the non-significant terms have been removed from the equation. The first-order variable with no significant P-value must remain in the model only if any of its second-order variables is significant. When the model has been created, residual analysis was performed to check its efficiency. The latter includes statistical calculation such as residual plots and residual standard deviation, in which the accuracy of the selected regression can be graphically appraised. The response surface graph can be drawn once the accuracy of the model is validated [31].

The significance of the model was determined by performing an analysis of variance (ANOVA) using the language for statistical computing R [30], where the results are given in Table 5. F-test and P-value were used to determine the significance of the model. P-values lower than 0.0001 were obtained for all the models, implying that the models are significant.

The validation of the regression models included the determination coefficient ( $R^2$ ), the adjusted coefficient of multiple determinations (Adj- $R^2$ ), the root means square error (RMSE), the F Statistic value, the lack-of-fit P-value, the model P-value, and the Shapiro-Wilk P-value given in Table 5. The models presented a high determination coefficient ( $R^2$ ), explaining 97%, 96%, 96% and 95% of the variability in the responses  $\bar{\varnothing}_m$ , R1, R7, and R28, respectively. This indicates an appropriate fit for the model and high statistical significance of the model. It shows that a high correlation exists between the experimental and predicted values. Furthermore, the adjusted  $R^2$  values are very close to the  $R^2$ , which shows that the unnecessary terms are not added in the model. Lack-of-fit test was run to check

Table 6.  
ANOVA results for fitted numerical models.

Model Terms	$\mathcal{O}_m$		R1		R7		R28	
	Coeff	P-value	Coeff	P-value	Coeff	P-value	Coeff	P-value
Inter.	240.616	<0.001	47.099	<0.001	95.149	<0.001	148.753	<0.001
A	-1.659	0.019	1.082	0.239	0.785	0.351	3.462	<0.001
B	21.206	<0.001	-2.253	0.028	-2.237	0.022	-1.747	0.005
C	6.119	<0.001	-8.224	<0.001	-4.938	<0.001	5.645	<0.001
A:B	3.344	0.050	-2.669	0.046	4.392	0.003	-	-
A:C	-	-	-4.863	0.002	-4.073	0.005	-	-
B:C	-2.969	0.049	-11.436	<0.001	-7.083	<0.001	2.336	0.005
A:B:C	-	-	-	-	-	-	3.006	<0.001
$A^2$	2.945	0.021	-	-	3.096	0.004	-1.179	0.025
$B^2$	-	-	-1.651	0.071	5.307	<0.001	-	-
$C^2$	-	-	-4.142	<0.001	2.764	0.007	-	-

Source: The Authors.

the goodness of the regression model. The optimal value of lack-of-fit is zero. All the P-values calculated in the ANOVA process purported that the lack-of-fit is not significant compared to the pure error. In addition, the Shapiro-Wilk test showed P-values higher than 0.05 in all cases.

### 3.2. Analysis of factors using response surface methods

The developed response surface methodology models are checked through ANOVA by analyzing the effect of individual parameters and their interactions on responses. The significant parameters were detected by *t-test* by determining which of them had P-value below the threshold value of 0.05, which indicates that their contribution improves the model. Table 6 depicts the estimation parameter of the models (model terms) and their corresponding P-values. Parameters with a P-value higher than 0.05 were not considered in model, except for the aforementioned exception. The response surface can be plotted by presenting the response as a function of three factors, in triangular graphics. Figs. 5-8 shows the contour and the response surface plots in the domain region in function of factors A (Cement content in kg), B (water to binder ratio) and C (superplasticizer content in volume). These plots provide information on the effect of the three independent components on average spread ( $\mathcal{O}_m$ ) and compressive strength with standard curing conditions at 24 hours (R1), 7 days (R7), and 28 days (R28).

### 3.3. Spread flow

The effect of variation of factors A, B and C on average spread ( $\mathcal{O}_m$ ) is shown in Fig. 5. According to ANOVA results, presented in Table 6, a linear relation was obtained between the spread length and the water to binder ratio, which is the most significant factor. According to EFNARC [32], a spread flow value from 240 to 260 mm is considered adequate for a plain self-consolidated concrete (SCC). The addition of cement and powders generally resulted in a higher viscosity of the mixtures and, therefore, the value of spread flow decreased with the increase of cement (factor A). As expected, the water to binder ratio (factor B) and superplasticizer content (factor C) have a positive effect on the spread flow value. Water to binder ratio has the most

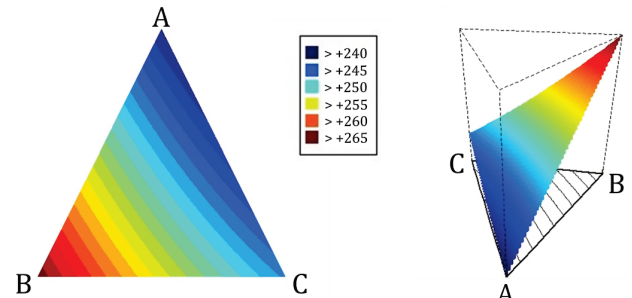


Figure 5. Response surface 2D-3D plots indicating interaction effects of the amount of cement (A), w/b ratio (B) and superplasticizer content (C) on the spread flow.

Source: The Authors.

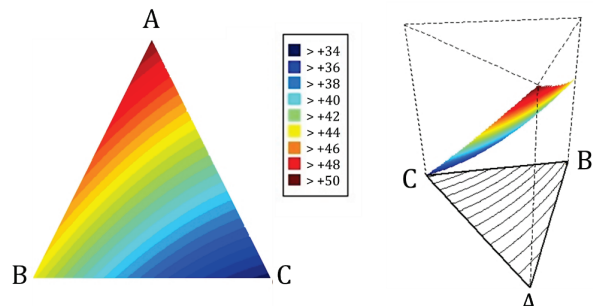


Figure 6. Response surface 2D-3D plots indicating interaction effects of factors A, B, and C on the 1-day compressive strength.

Source: The Authors.

influence in this field, however, its implications in compressive strength, and superior threshold, forces us to limit its use.

### 3.4. 1-day compressive strength

The effect of three-factor on 1-day compressive strength is monitored as a contour plot and 3-D plot in Fig. 6. The maximum value corresponds to the maximum level (1) of cement (A). According to ANOVA results, presented in Table 6, a nonlinear relationship was obtained between the 1-day compressive strength and the three factors. As shown in Fig. 6, the early compressive strength increases with the increase of cement (A) but increases much more with a decrease in water to binder ratio (B) and superplasticizer content (C). The negative effect of the increasing water in the compressive strength is a well-known effect. Even the negative effect of polycarboxylate on early strength development has been demonstrated by several researchers [34,35]. The polycarboxylate based ether superplasticizer slows down the hydration of silicates (especially the alite phase and also affects the formation of ettringite) [33].

### 3.5. 7-day compressive strength

Fig. 7 shows the contour and 3D plot of the effect of factors A, B, and C on the 7-days compressive strength. The

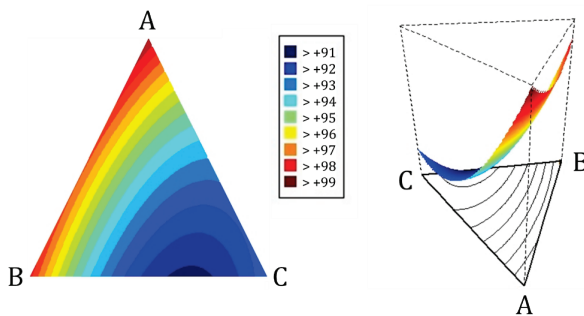


Figure 7. Response surface 2D-3D plots indicating interaction effects of factors A, B, and C on the 7-day compressive strength.  
Source: The Authors.

maximum value of 7-day compressive strength could be seen when factor A value is at its maximum level (1) and factor C is at a minimum level (-1). As for 1-day compressive strength, according to ANOVA results, presented in Table 6, a nonlinear relationship was obtained between the 7-day compressive strength and the three factors studied.

### 3.6. 28- day compressive strength

The effect of variables on 28-day compressive strength is shown in Fig. 8 as a 3D plotting. It shows the positive effect of variables on the 28-day compressive strength of UHPC as cement and superplasticizer in the highest level (1) while water to binder ratio remains in the lower level (-1), giving the maximum 28-day compressive strength.

The effect of superplasticizer content on 28 compressive strength is provided in Fig. 8. It shows that, contrary to what happens with early strength, by increasing the superplasticizer content, the 28-day compressive strength rate increases.

Once again, the nonlinear relationship was obtained between the 28-day compressive strength and the three factors studied.

### 3.7. Model Checking

Generally, a model's adequacy is investigated through the examination of residuals. For the model to be adequate, the pattern of residual plots should be structureless.

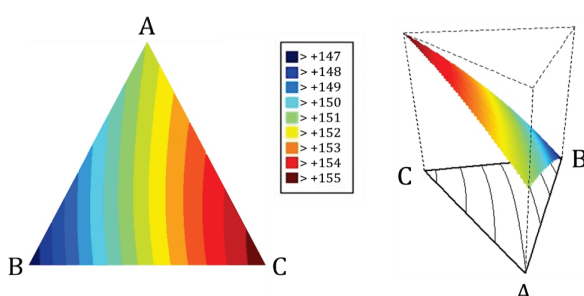


Figure 8. Response surface 2D-3D plots indicating interaction effects of factors A, B, and C on the 28-day compressive strength.  
Source: The Authors.

The normal probability plot of the residuals of each RSM (Fig. 9) shows that the residuals lie reasonably close to a straight line, implying that errors are distributed normally and supporting the claim that the terms mentioned in the model are significant.

A graph of the predicted response values versus the actual response values is shown in Fig. 10. It helps to detect a value, or group of values, that are not easily predicted by the model.

The figure also shows any abnormalities in response.

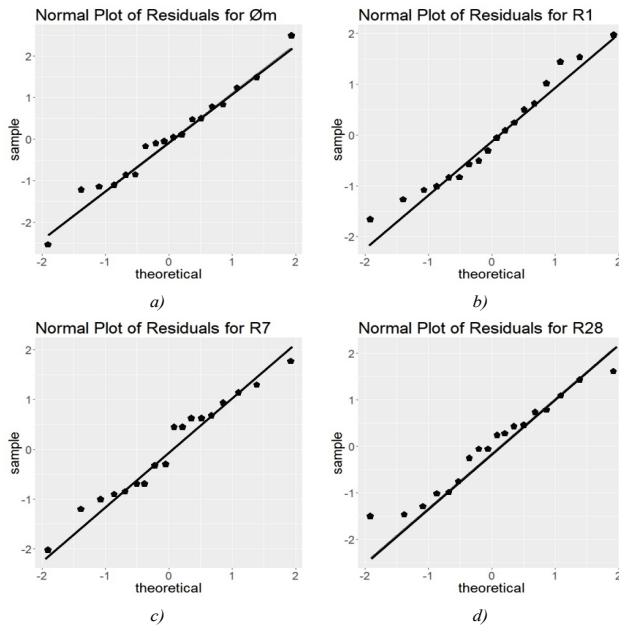


Figure 9. Normal Plot of residuals for each response's model: a) Øm; b) R1; c) R7; and d) R28.  
Source: The Authors.

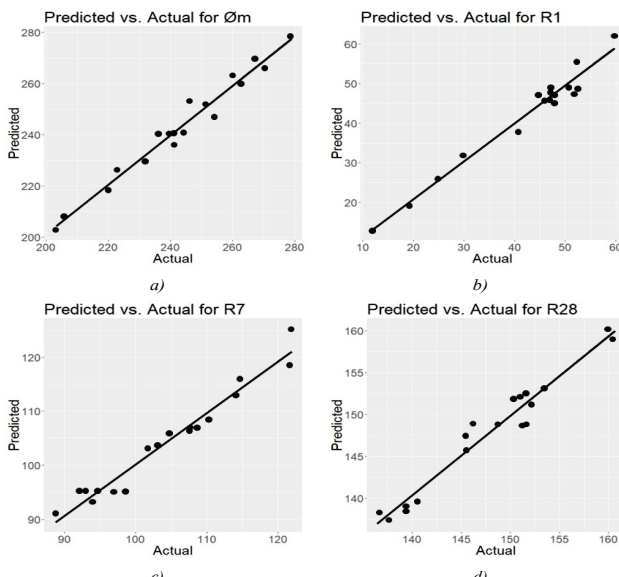


Figure 10. Predicted versus Actual values for each response's model: a) Øm; b) R1; c) R7; and d) R28.  
Source: The Authors.

## 4. Multi-objective optimization of RPC

### 4.1. Methodology

A multi-objective optimization R-coded algorithm [21] was employed, aimed at settling the optimum values for the independent variables that can reach the best value for the response. The algorithm was based on the multiple response optimization introduced by Derringer and Suich in 1980 [35]. The methodology translated each response function into a desirability function and maximized the geometric mean of the desirability of each response by using single objective optimization technique. First step is establishing a numerical model between factors and responses. Then all independent variables were sorted simultaneously and independently to optimize the objective responses. This optimal solution aims to accomplish the requirements for each of the responses keeping a balance among them [27].

The geometric mean of individual desirability is shown in eq. (5) [35].

$$D = (d_1^{r_1} \times d_2^{r_2} \times d_3^{r_3} \times \dots \times d_n^{r_n})^{1/\sum r_i} = \left[ \prod_{i=1}^n d_i^{r_i} \right]^{1/\sum r_i} \quad (5)$$

where  $d_i$  is a desirability of each response,  $r_i$  is the weight or importance of each response, and  $n$  is the number of responses included in the optimization. Weight ( $r_i$ ) varies from 1 (least important) to 5 (most important).  $d_i$  is the individual desirability function of a response, which ranges from 0 (undesired response) to 1 (fully desired response). Thus, the individual desirability function can convert the value of a response into a value between 0 and 1. The final value of  $D$  is a value between 0 and 1. For perfect accomplishment of the target values, the value of  $D$  is unity.

Due to the nature of eq. (5) if any of the responses is outside its desirability range, the overall function becomes zero.

The individual desirability function form of each response for minimization, maximization and in range cases is shown in eqs. (6), (7) and (8), respectively.

$$d = \begin{cases} 1 & Y_i \leq L \\ \left[ \frac{U - Y_i}{U - L} \right]^{wt_i} & L < Y_i < U \\ 0 & Y_i \geq U \end{cases} \quad (6)$$

$$d = \begin{cases} 0 & Y_i \leq L \\ \left[ \frac{Y_i - L}{U - L} \right]^{wt_i} & L < Y_i < U \\ 1 & Y_i \geq U \end{cases} \quad (7)$$

$$d = \begin{cases} 0 & Y_i \leq L \\ 1 & L < Y_i < U \\ 0 & Y_i \geq U \end{cases} \quad (8)$$

where  $U$  is an upper limit,  $L$  is a lower limit for a response, and  $wt_i$  is the weight or shape of the function. Using different weights, the shape of the individual desirability for each target can be changed. The  $wt_i$  value varies between 0.1 and 10. Values greater than 1 give more importance to the goal,

Table 7.

Optimization of the individual responses for a self-compacting UHPC mixture with high 28 days compressive strength (Criteria I) and with minimum cement content (Criteria II).

Responses and variables	Lower	Upper	Criteria I		Criteria II	
			Goal	Importance	Goal	Importance
$\bar{\Omega}_m(\text{mm})$	240	260	In range	5	In range	5
R28(MPa)	150	165	Maximum	5	Maximum	5
C( $\text{kg}/\text{m}^3$ )	600	650	-	-	Minimum	5

Source: The Authors.

Table 8.

Optimum mixtures for Criteria I and Criteria II.

Mix	A	B	C	Desirability
Criteria I	Coded	1.19	-0.149	1.7889
	Real	654.81	0.164	0.0256
Criteria II	Coded	-0.149	-0.149	1.7889
	Real	621.27	0.164	0.0256

Source: The Authors.

Table 9.

Experimental measurement responses versus predicted by model.

Mix	$\bar{\Omega}_m(\text{mm})$	ARD%	R28 (MPa)		ARD%
			Experimental	Model	
Criteria I	246.50	250.28	1.51%	160.28	163.28 1.60%
Criteria II	253.00	250.35	1.05%	158.32	158.32 1.24%

Source: The Authors.

having the weight values lower than 1 prompt the opposite effect. A weight of 1 implies that  $d_i$  varies in a linear way. In this work, the multi-objective optimization process was performed in two consecutive steps, in which responses and factors were defined as a specific target by assigning a specific level of importance. Table 7 shows the goals of both optimization criteria for each response. Criteria I has been presented for selecting the optimum factor values to obtain a self-compacting mixture according to EFNARC criteria [32] with the maximum 28-days compressive strength. In this study, the slump flow was defined as ‘in range’ goal, while 28-days compressive strength was defined as ‘maximum’ goal. Once the optimization process is finished, one optimal solution, accomplishing the specified constraints was obtained. Criteria II adds to Criteria I the desire for minimum content of cement, maintaining a 28-days compressive strength over 150 MPa. In this work, the three responses: compressive strength, slump flow and cement content are considered equally important. Both optimized mixtures are shown in Table 8.

### 4.2. Experimental validation

The efficiency of the mathematical-selected dosages was evaluated by carrying out the experiment under optimal conditions and by comparing obtained predicted values with the two mixtures presented in Table 8. Table 9 shows the absolute relative deviation between model and experimental values, ARD (%), which is used as a measure of

predictability a toll for validation. The results confirmed that the experimental values are close to the values predicted by the multi-objective optimization.

It is important to note that the mixture designed under Criteria II and tested experimentally, resulted in a reduction of cement content of approximately 22%, and of silica fume by over 50%, compared to the typical dose of RPC proposed by Richard and Cheyrezy [1]. These partial substitutions for less expensive materials such as recycled glass, EASF and limestone powders, leads to a reduction in the final cost of the mixture of approximately 20%, while maintaining the compressive strength above 150 MPa.

## 5. Conclusions

In this work, a reactive powder concrete using by-products as cementitious supplementary materials, such electric arc slag furnace, and recycled glass powder, in addition to limestone powder was obtained through a multi-objective simultaneous optimization. In this model, the factorial design and the response surface method (RSM) were incorporated. Five responses, spread flow, the compressive strength at 1,7 and 28 days, and cement content, were studied, while using three of them (compressive strength, slump flow and cement content) in the optimization mixture design method. Based on the results of this experimental investigation, the following conclusions were drawn:

1. An optimal mixture was designed to reach 150 MPa at 28-days compressive strength with only 621 kg/m<sup>3</sup> of HE cement and 100 kg/m<sup>3</sup> of silica fume. This provides an RPC, which incorporates by-products in its dosage such as electric arc slag furnace and recycled glass flour.
2. The proposed numerical models provide an accurate examination of RPC properties over the selected range of cement content, water to binder ratio and superplasticizer content. The high values for coefficients of multiple determinations ( $R^2$ ) combined with lack-of-fit test results demonstrated the accuracy of the second-order model to predict the behaviour of RPC in relation to compressive strength at 1, 7 and 28 days, as well as spread flow value. ANOVA tests also confirmed the inclusion of all model's parameters which are statistically significant, due to their low P-value.
3. Regarding rheological properties, water-to-binder ratio has a positive effect, nevertheless it has negative effect on strength of all ages of concrete. The superplasticizer content has a positive effect on the slump flow. However, polycarboxylate content has a negative effect on the early-strength but a positive effect on the 28-day compressive strength.
4. The study of results predicted by the model compared to those obtained in the experiments leads to the conclusion that the statistical model can be used to predict properties for new mixtures with good accuracy.

## Acknowledgments

Special thanks to Cementos Argos SA. for donating most

of the materials used in the research. The supply of recycled glass from Cristalería Peldar SA and EASF form GERDAU SA for this research is highly appreciated. The writers would also like to acknowledge the support and suggestions of the Escuela Colombiana de Ingeniería Julio Garavito and the Polytechnic University of Madrid (UPM).

## References

- [1] Richard, P. and Cheyrezy, M., Composition of reactive powder concretes. *Cem. Concr. Res.*, 25(7), pp. 1501-1511, 1995.
- [2] Song, J. and Liu, S., Properties of reactive powder concrete and its application in highway bridge, *Adv. Mater. Sci. Eng.*, 2016, 2016. DOI: 10.1155/2016/5460241
- [3] Abbas, S., Nehdi, M.L. and Saleem, M.A., Ultra-High performance concrete: mechanical performance, durability, sustainability and implementation challenges, *Int. J. Concr. Struct. Mater.*, 10(3), pp. 271-295, 2016. DOI: 10.1007/s40069-016-0157-4
- [4] Jammes, F., Cespedes, X. and Resplendino, J., Design of Offshore wind turbines, RILEM-fib-AFGC Int. Symp. Ultra-High Perform. Fibre-Reinforced Concr. UHPFRC 2013(1), pp. 443-452, 2013.
- [5] Taguit-Hamou, A., Soliman, N.A. and Omran, A., Green Ultra-high-performance glass concrete, First International Interactive Symposium on UHPC, 3(1), pp. 1-10, 2016. DOI: 10.21838/uhpc.2016.35
- [6] De Larrard, F. and Sedran, T., Mixture-proportioning of high-performance concrete, *Cem. Concr. Res.*, 32(11), pp. 1699-1704, 2002. DOI: 10.1016/S0008-8846(02)00861-X
- [7] Meng, W., Samaranayake, V.A. and Khayat, K.H., Factorial design and optimization of UHPC with lightweight sand, *ACI Mater. J.*(February), 2018. DOI: 10.14359/51700995
- [8] Abdulkareem, O.M., Ben Fraj, A., Bouasker, M. and Khelidj, A., Effect of chemical and thermal activation on the microstructural and mechanical properties of more sustainable UHPC, *Constr. Build. Mater.*, 169, pp. 567-577, 2018. DOI: 10.1016/j.conbuildmat.2018.02.214
- [9] Ghanem, H. and Obeid, Y., The Effect of steel fibers on the rheological and mechanical properties of self compacting concrete, *Eur. Sci. J.*, 11(21), pp. 85-98, 2015.
- [10] Li, W., Huang, Z., Zu, T., Shi, C., Duan, W.H. and Shah, S.P., Influence of Nanolimestone on the hydration, mechanical strength, and autogenous shrinkage of ultrahigh-performance concrete, *J. Mater. Civ. Eng.*, 28(1), pp. 1-9, 2016. DOI: 10.1061/(ASCE)MT.1943-5533.0001327
- [11] Huang, Z. and Cao, F., Effects of nano-materials on the performance of UHPC, *材料导报 研究篇*, 26(9), pp. 136-141, 2012.
- [12] Camacho, E., López, J.A. and Serna, P., Definition of three levels of performance for UHPFRC-VHPFRC with available materials, in: Proceedings of Hipermat 2012, 3<sup>rd</sup> International Symposium on UHPC and Nanotechnology for Construction Materials, Kassel Uni., Kassel, Germany, 2012, pp. 249-256.
- [13] Camacho-Torregosa, E., Dosage optimization and bolted connections for UHPFRC ties, PhD Thesis, Polytechnic University of Valencia, Spain, 2013.
- [14] Van Tuan, N., Ye, G., Van Breugel, K., Fraaij, A.L.A. and Danh, B., The study of using rice husk ash to produce ultra high performance concrete, *Constr. Build. Mater.*, 25(4), pp. 2030-2035, 2011. DOI: 10.1016/j.conbuildmat.2010.11.046
- [15] Van Tuan, N., Ye, G. and Van Breugel, K., Mitigation of early age shrinkage of ultra high performance concrete by using rice husk ash, in: Proceedings of Hipermat 2012, 3<sup>rd</sup> International Symposium on UHPC and Nanotechnology for Construction Materials., Kassel Uni., 2012, pp. 341-348.
- [16] Soliman, N.A. and Taguit-Hamou, A., Partial substitution of silica fume with fine glass powder in UHPC: filling the micro gap. *Constr. Build. Mater.*, 139, pp. 374-383, 2017. DOI: 10.1016/j.conbuildmat.2017.02.084
- [17] Soliman, N.A. and Taguit-Hamou, A., Using glass sand as an alternative for quartz sand in UHPC, *Constr. Build. Mater.*, 145, pp. 243-252, 2017. DOI: 10.1016/j.conbuildmat.2017.03.187

- [18] Yu, R., Tang, P., Spiesz, P. and Brouwers, H.J.H., A study of multiple effects of nano-silica and hybrid fibres on the properties of Ultra-High Performance Fibre Reinforced Concrete (UHPFRC) incorporating waste bottom ash (WBA), *Constr. Build. Mater.*, 60(June), pp. 98-110, 2014. DOI: 10.1016/j.conbuildmat.2014.02.059
- [19] Yu, R., Spiesz, P. and Brouwers, H.J.H., Mix design and properties assessment of Ultra-High Performance Fibre Reinforced Concrete (UHPFRC), *Cem. Concr. Res.*, 56, pp. 29-39, 2014. DOI: 10.1016/j.cemconres.2013.11.002
- [20] Funk, J.E. and Dinger, D., Predictive process control of crowded particulate suspensions: applied to ceramic manufacturing, Springer Science, New York, USA, 1994.
- [21] Roth, T., Working with the quality. Tools package, 2016. [Online]. Available at: <http://www.r-qualitytools.org>.
- [22] Abellán, J., Torres, N., Núñez, A. y Fernández, J., Influencia del exponente de Fuller, la relación agua conglomerante y el contenido en policarboxilato en concretos de muy altas prestaciones, en: IV Congreso Internacional de Ingeniería Civil, La Habana (Cuba), 2018.
- [23] ASTM, 'Standard test method for flow of hydraulic cement mortar,' American Society for Testing and Materials C1437. Conshohocken, PA, USA, 2016, pp. 1-2.
- [24] ASTM, 'Standard Test method for compressive strength of hydraulic cement mortars (Using 2-in. or [50-mm] cube specimens),' American Society for Testing and Materials C109/C109M - 11b. West Conshohocken, PA, USA, 2010, pp. 1-9.
- [25] Lenth, R.V., Response-surface methods in R, using rsm, *J. Stat. Softw.*, 32(7), pp. 1-17, 2012.
- [26] Raviselvan, R.J., Ramanathan, K., Perumal, P. and Thansekhar, M.R., Response surface methodology for optimum hardness of TiN on steel substrate, *Int. J. Chem. Mol. Nucl. Mater. Metall. Eng.*, 9(12), pp. 1331-1337, 2015.
- [27] Ghafari, E., Costa, H., Nuno, E. and Santos, B., RSM-based model to predict the performance of self-compacting UHPC reinforced with hybrid steel micro-fibers, *Constr. Build. Mater.*, 66(September), pp. 375-383, 2014. DOI: 10.1016/j.conbuildmat.2014.05.064
- [28] Abellán, J., Fernández, J.A., Torres, N. and Núñez, A.M., Statistical Optimization of ultra-high-performance glass concrete, *ACI Mater. J.*, 117(M), pp. 243-254, 2020. DOI: 10.14359/51720292
- [29] Branchu, S., Forbes, R.T., York, P. and Nyqvist, H.N., A central composite design to investigate the thermal stabilization of lysozyme, *Pharmaceutical Research*, 16(5), pp. 702-708, 1999. DOI: 10.1023/a:1018876625126
- [30] R Core Team, R: A Language and Environment for Statistical Computing. Vienna, Austria, 2018.
- [31] Montgomery, D.C., Design and analysis of experiments. John Wiley & Sons, Inc, New Jersey, USA, 2005.
- [32] The European Project Group, 'The European Guidelines for Self-Compacting Concrete,' *Eur. Guidel. Self Compact. Concrete*, (May), 2005, 63 P.
- [33] Puertas, F., Santos, H., Palacios, M. and Martínez-Ramírez, S., Polycarboxylate superplasticiser admixtures: effect on hydration, microstructure and rheological behaviour in cement pastes, *Adv. Cem. Res.*, 17(2), pp. 77-89, 2005. DOI: 10.1680/adcr.17.2.77.65044
- [34] Kubens, S., Interaction of cement and admixtures and its influence on rheological properties, [online]. 49(0), Göttingen, 2010. Available at: <https://cuvillier.de/de/shop/publications/752>
- [35] Derringer, G. and Suich, R., Simultaneous Optimization of several response variables. *J. Qual. Technol.*, 21(4), pp. 214-219, 1980. DOI: 10.1080/00224065.1980.11980968

**A. Núñez-López**, is a Civil Engineer at Cementos Argos SA, Medellín, Colombia. He received his BSc. in civil engineering from the Universidad del Quindío, Colombia; his MSc. from the Polytechnic University of Valencia, Spain; and his PhD. in civil engineering from the Polytechnic University of Valencia, Spain.  
ORCID: 0000-0001-5811-4818

**Nancy Torres-Castellanos**, is a Professor of civil engineering at Escuela Colombiana de Ingeniería Julio Garavito, Bogotá, Colombia. She received her BSc. in civil engineering in the Universidad Francisco de Paula, Santander, Colombia; her MSc. in structural engineering from the Universidad Nacional de Colombia, and her PhD. in engineering science and technology of materials from the Universidad Nacional de Colombia.  
ORCID: 0000-0003-3293-5444

**Jaime Fernández-Gómez**, is Professor in the Department of Civil Engineering: Construction at the Polytechnic University of Madrid (UPM), Madrid, Spain. He received his BSc. in civil engineering and PhD. in civil engineering from the Polytechnic University of Madrid (UPM), Madrid, Spain. His research interests include structural analysis, construction engineering, and civil engineering materials.  
ORCID: 0000-0001-9894-4357



**UNIVERSIDAD NACIONAL DE COLOMBIA**  
 SEDE MEDELLÍN  
 FACULTAD DE MINAS

**Área Curricular de Ingeniería Civil**

**Oferta de Posgrados**

**Doctorado en Ingeniería - Ingeniería Civil**  
**Maestría en Ingeniería – Estructuras**  
**Maestría en Ingeniería – Geotecnia**  
**Maestría en Ingeniería - Infraestructura y Sistemas de Transporte**  
**Especialización en Estructuras**  
**Especialización en Ingeniería Geotecnia**  
**Especialización en Vías y Transportes**

Mayor información:  
 E-mail: [asisacim@unal.edu.co](mailto:asisacim@unal.edu.co)  
 Teléfono: (57-4) 425 5172

**J. Abellán-García**, is a PhD. candidate of the Department of Civil Engineering at the Polytechnic University of Madrid (UPM), Madrid, Spain. He received a BSc. Eng. in Civil Engineering in 2006 from the Polytechnic University of Valencia (UPV), a MSc. in Railway Infrastructure, in 2010 from the Polytechnic University of Catalonia (UPC), Spain. He is also professor of civil engineering at Escuela Colombiana de Ingeniería Julio Garavito, Bogotá, Colombia. His research interests include mathematical optimization of eco-friendly ultra-high-performance concrete and seismic behavior of high strain hardening cementitious composites.  
ORCID: 0000-0002-0353-322X